Journal of Science and Transport Technology
Journal homepage: https://jstt.vn/index.php/en

UNIVERSITY OF TRANSPORT TECHNOLOGY

Effect of Groove Geometry on Stress Distribution and Fatigue Life of TC4 Alloy

Le Thi Tuyet Nhung[1,*], Le Minh Duc[1,*], Nguyen The Hoang[2]
[1]School of Mechanical Engineering, Hanoi University of Science and Technology, 1 Dai Co Viet, Hanoi, 100000, Vietnam
[2]Aviation Management - BCD, Singapore Institute of Technology, Singapore; thehoang.nguyen@singaporetech.edu.sg

Article info
Type of article:
Original research paper

DOI:
https://doi.org/10.58845/jstt.utt.2026.en.6.3.258-274

***Corresponding author:**
Email address:
nhung.lethituyet@hust.edu.vn
duc.lm241271e@sis.hust.edu.vn

Received: 11/05/2026
Received in Revised Form: 22/06/2026
Accepted: 12/07/2026

Abstract: In this study, the fatigue life prediction simulation of Chen et al. for TC4 titanium alloy components with surface defects is reconstructed and validated. When a scratch defect with a depth of 0.25 mm is introduced into the simulation, stress concentration occurs at the scratch root, and the predicted fatigue life reaches 3.2×10^5 cycles, with an error of approximately 8% compared to the reference results. Based on this validation, the study is extended to investigate the influence of groove geometry on stress distribution and fatigue life using a dimensionless geometric parameter, i_{AR}. The results show that as i_{AR} increases, the maximum von Mises stress at the groove root decreases significantly, leading to a nonlinear increase in fatigue life. For i_{AR} < 2.7, the fatigue life remains lower than that of the initial component, whereas for values exceeding this threshold, the fatigue life is restored and significantly improved.

Keywords: Fatigue life; TC4 alloy; Surface defects.

1. Introduction

TC4 titanium alloy (Ti-6Al-4V) is one of the most important metallic materials in the fields of aerospace, defense, and mechatronics due to its high strength-to-weight ratio, excellent corrosion resistance, and stability under harsh environmental conditions. However, under cyclic loading, especially in components requiring high reliability such as transmission systems, blades, joints, or vibration-prone structures, this material still presents a risk of fatigue crack initiation and propagation. Small-scale surface defects, such as scratches generated during machining, assembly, or wear, can act as initiation sites for cracks, thereby significantly reducing the service life of the structure. In addition, various factors such as microstructural characteristics, load ratio, multiaxial loading, environmental conditions, and high loading rates have also been shown to significantly influence the mechanisms and growth rate of fatigue cracks.

In this context, the accurate evaluation of fatigue life plays an important role in ensuring the reliability and safety of structures. Therefore, in recent years, numerous studies have focused on the evaluation and prediction of the fatigue life of TC4 alloy under different loading conditions and material characteristics, among which several works have also considered the role of crack initiation mechanisms as a governing factor in the overall fatigue life of components.

In the study by Aniket Mote et al. (2024) [1], the authors focused on investigating specimens with various sizes and load ratios to evaluate the influence of loading conditions and specimen configuration on crack growth characteristics. The study analyzed the relationship between crack growth rate and the stress intensity factor by applying and comparing multiple testing procedures. The results showed that conventional load-shedding methods are significantly affected by loading history and crack closure effects, leading to an overestimation of the threshold value ΔKth as well as deviations in crack growth rates. In contrast, methods based on compression pre-cracking, particularly CPCA, provide more stable results that are in better agreement with the predictions of the FASTRAN crack-closure model, thereby offering a more reliable approach for determining fatigue characteristics in the near-threshold regime. Previously, the effects of fracture toughness and crack closure on the crack growth rate relationship da/dN-ΔK were investigated by V. Sinha (2000) [2] and Zhang Junhong et al. (2015) [3]. In the study by V. Sinha (2000) [2], fatigue crack growth behavior in Ti-6Al-4V was examined experimentally in detail. The research employed fatigue tests on CT and SEN specimens, combined with crack closure measurements and microstructural observation techniques to analyze crack propagation mechanisms. The results showed that short cracks can propagate at stress intensity factor levels lower than the threshold for long cracks. This difference is mainly attributed to the lower degree of crack closure in short cracks. When corrected for crack closure effects, the data for short and long cracks tend to converge, indicating that crack closure plays a key role in accurately describing the fatigue behavior of the material. ZHANG Junhong et al. (2015) [3] also addressed crack closure as a factor influencing crack growth rate and proposed a new fatigue life prediction formulation. In this study, experiments including fracture toughness measurements and fatigue crack growth investigations were conducted on notched specimens under various loading conditions. Based on the experimental data, the authors developed a crack growth rate prediction approach that incorporates the effect of crack closure and introduces a correction factor to describe the relationship between the stress intensity factor range and fracture toughness.

The influence of microstructure on fatigue life and crack propagation has also been a widely studied topic. In the study by Gou Ping et al. (2015) [4], the fatigue crack growth behavior of TC4-DT titanium alloy with different lamellar microstructures, produced through various heat treatment conditions, was investigated in detail. The study focused on Ti-6Al-4V alloy specimens with variations in lamellae thickness, colony size, and grain size. Through mechanical experiments combined with microstructural observations, the study analyzed the influence of microstructural characteristics on crack propagation mechanisms, showing that parameters such as lamellae thickness and colony size play a decisive role in fracture toughness and crack growth rate. In particular, the microstructure obtained by air cooling from the β phase region exhibits the highest resistance to fatigue crack propagation due to the formation of a larger plastic zone at the crack tip.

The environment is also one of the key factors governing the initiation of fatigue cracks. Stuart R. Stock and Morten A. Langøy (2001) [5] investigated the fatigue crack growth behavior of Ti-6Al-4V-0.1Ru titanium alloy, applied to riser pipes in offshore oil and gas operations. The study focused on evaluating the effects of environmental and loading conditions such as temperature, frequency, load ratio, seawater environment, and strain state on crack growth rate. The results showed that load ratio and frequency are the most influential factors on crack growth rate, whereas temperature and seawater environment have only a minor effect.

One of the prominent research directions in recent years is the combination of TC4 with other materials to enhance the mechanical properties of components [6-9]. In these studies, TC4 is typically integrated with alloys such as TB8, TC17, and TA15 through various fabrication methods, including laser melting deposition, diffusion bonding… Subsequently, fatigue tests are conducted in conjunction with microstructural analysis to clarify the interaction mechanisms as well as the resulting improvements in material properties. This approach not only helps overcome the inherent limitations of TC4 but also contributes to improving overall strength and expanding its application range under severe working conditions.

To enhance the fatigue life of components, various surface treatment methods have been investigated and proposed to improve the residual stress state, increase surface hardness, and suppress the initiation as well as the propagation of fatigue cracks [8, 10-12]. In the studies by Pengfei Li et al. (2026) [8] and Gao Jiayuan (2025) [10], despite differences in the investigated objectives, the results consistently demonstrate that the ultrasonic rolling process is effective in improving resistance to fatigue crack initiation. In addition, the works of Ping Zhang et al. (2025) [11] and Venkataramana et al. (2025) [12] have introduced different surface strengthening techniques applied to Ti-6Al-4V. These methods have been shown to reduce the influence of surface defects and delay crack propagation, thereby significantly extending the service life of the components.

The fatigue life of Ti-6Al-4V components fabricated by laser-arc hybrid welding has been investigated by Shengbo Li et al. (2026) [13] and Zheng Lei et al. (2026) [14]. In these studies, the authors consistently conclude that pore defects generated during the welding process are the primary factor leading to crack initiation and causing significant scatter in fatigue life data. However, the two works differ in their approaches and predictive methodologies. While Shengbo Li's study focuses on developing a damage evolution model through ABAQUS simulations to track material stiffness degradation, Zheng Lei's work further explores crack initiation mechanisms under varying stress levels and employs a Physics-Informed Neural Network (PINN) to predict fatigue life based on geometric parameters of the defects. The results of both studies demonstrate high accuracy, with Li's model falling within a factor of two error range, and Lei's PINN model achieving 97% of predictions within a factor of three error range.

Studies on the properties of TC4 under extremely severe working conditions have also been conducted in recent years. In the study by Hailong Deng et al. (2025) [15], the authors presented a comprehensive investigation into the fatigue behavior of TC4 within the very high cycle regime. By employing advanced microscopic techniques such as TEM and FIB, the study elucidated the mechanism of internal crack initiation through the interaction of dislocation structures. A key highlight of this work is the successful development of a fatigue life prediction framework that accounts for the maximum defect size. Ying Wang et al. (2026) [16] provided a comprehensive insight into the effect of temperature on the crack resistance of Ti-6Al-4V. By combining precise mechanical testing with microstructural analysis techniques such as SEM and EBSD, the study demonstrated that the simultaneous activation of multiple slip systems at elevated temperatures is the key factor enabling TC4 to achieve superior fracture toughness (increasing by 66% at 250°C).

When considering the practical applications of TC4 alloy, another important aspect to take into account in fatigue life assessment is the influence of surface defects. In the study by Xin Chen et al. (2024) [17], the damage tolerance of TC4 titanium alloy was investigated, with a focus on typical surface defects such as scratches and impact-induced dents. Through high-cycle fatigue tests, S-N curves were established for specimens with and without defects, combined with fracture surface analysis using microscopy techniques, the study clarified the influence of defect geometry on the fatigue behavior of the material. The results showed that the presence of defects significantly reduces the fatigue limit of TC4, with scratches having a more severe effect than dents due to higher stress concentration and the presence of multiple crack initiation sites. At the same time, the mechanisms of fatigue crack initiation and propagation were found to depend on both the type of defect and the stress level. From another perspective, Xulong Chen et al. (2026) [18] developed a method for evaluating the fatigue life of components in the presence of defects at critical locations, aiming to optimize computational time and cost. The study combines fatigue experiments and numerical analysis to clarify the mechanisms of crack initiation and propagation under the influence of scratches. And an equivalent fatigue life prediction simulation was proposed, in which the effect of scratches is incorporated through a stress amplification function, while also accounting for stress gradient effects and multiaxial stress states in the structure. The results show that cracks consistently initiate at the root of the scratch and that fatigue life decreases significantly as the scratch depth increases.

In addition to evaluating the initial defect tolerance of materials, practical applications also require consideration of the effects of post-repair damage, particularly surface grooves formed during crack removal by grinding. This leads to the need for reassessing the fatigue life of components after repair to determine their reusability. Mingchao Ding et al. (2022) [19] focused on predicting the fatigue life of TC4 titanium alloy in the presence of surface notch defects, which are commonly formed after crack removal on compressor blades. The study combined tensile fatigue experiments with elastic-plastic finite element analysis to analyze the local stress-strain distribution at the notch root. Based on this, a fatigue life prediction method was developed by integrating the Local Stress-Strain Approach (LSSA) to determine crack initiation life and fracture mechanics to describe crack propagation. The results showed that notch depth has a dominant influence on fatigue life, while increasing notch width can significantly improve fatigue life. In particular, the total fatigue life model achieved high accuracy, with prediction errors within a factor of 1.5.

A synthesis of recent studies indicates that the fatigue life and crack propagation behavior of TC4 alloy are influenced by multiple factors, including loading conditions, microstructural characteristics, service environment, and crack closure effects. In addition, surface defects, both in the initial state and after repair, have been shown to play a crucial role in crack initiation and propagation mechanisms. Current approaches primarily focus on combining experimental investigations with numerical modeling to improve the accuracy of fatigue life prediction while reducing computational cost. Although numerous studies have investigated crack growth behavior and fatigue life in TC4 components, as well as some works assessing reusability after crack removal by grinding, most existing studies are still limited to simple geometric configuration. Therefore, the effects of defects and repair processes on the fatigue life of thin-walled structures have not yet been fully clarified.

In this study, the fatigue life of TC4 components with defects in thin-walled structures is analyzed, and the reusability after crack removal by grinding is evaluated. Specifically, the study investigates the effect of locally enlarging the geometry at the defect location on the stress distribution and fatigue life of the component. Through numerical simulations, the study assesses the potential for reducing stress concentration and restoring fatigue life by modifying the defect geometry, thereby clarifying the effectiveness of local material removal as an approach to extend service life and reduce costs in practical engineering applications.

2. Validation

To evaluate the reliability of the numerical simulation approach used in this study, the fatigue life prediction model proposed by Chen et al. [18] is first reconstructed and validated using ANSYS Workbench. The validation focuses on the model's ability to reproduce the local stress field and fatigue life of components with and without surface defects, through comparison with published results. This model serves as a reference basis for subsequent analyses on the influence of defect geometry presented in the following sections.

2.1. CAD Model

Based on the geometry provided in Chen's study (Fig. 1), the CAD model was reconstructed using SolidWorks for validation purposes, as shown in Fig. 2. The component was partitioned into smaller sections to facilitate control and simplify the discretization process. A refined partitioning was applied in regions suspected of stress concentration. The case without cracks was analyzed first to verify the accuracy of the model against the reference study.

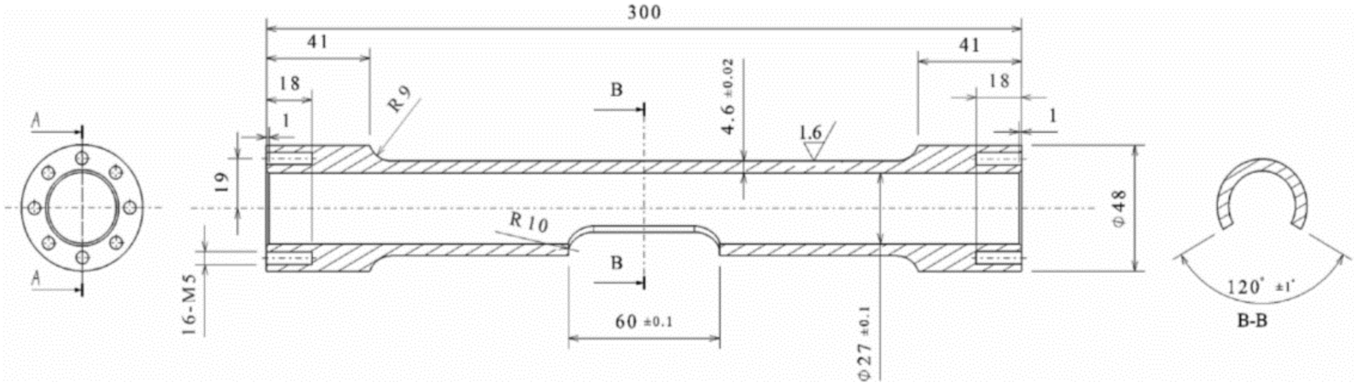

Fig. 1. Component schematic [18]

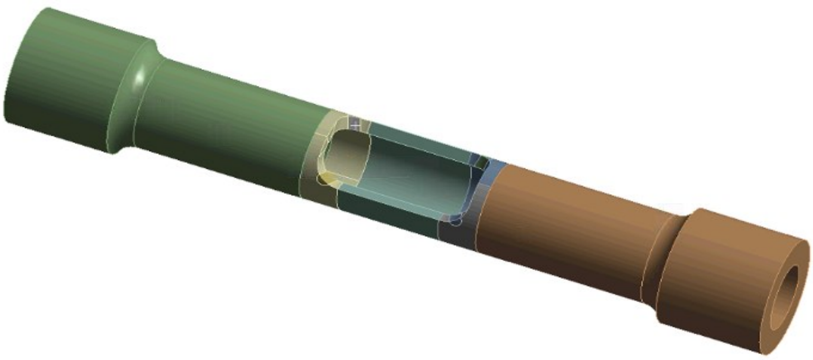

Fig. 2. Reconstructed component

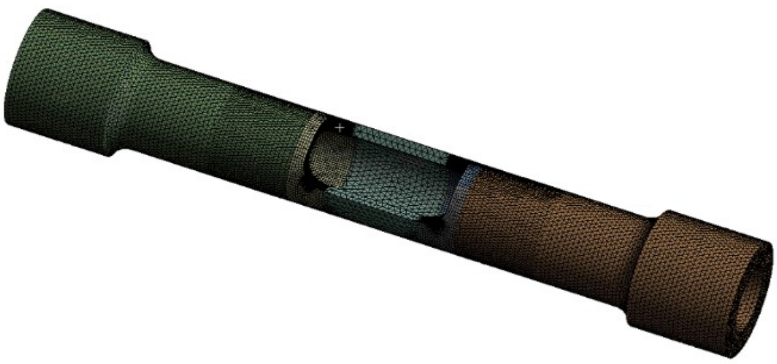

Fig. 3. Meshing result

2.2. Meshing

Based on the reconstructed CAD model, the geometry was partitioned and assigned region-specific element sizes prior to mesh generation for simulation. Due to the defect depth of h=0.25 mm, the region near the edge was expected to exhibit stress concentration, and therefore a refined mesh was applied. The element size in this region was set to approximately 0.1 mm, and gradually increased to about 0.25-3 mm away from the stress concentration zone to balance accuracy and computational cost, resulting in a mesh with high density near the defect and coarser elements toward the model boundaries. The total number of elements was approximately 450,000. The meshing results are illustrated in Fig. 3, clearly showing the refined mesh region around the defect and the coarser mesh toward the outer regions of the model.

2.3. Material properties

The material properties of TC4 were obtained from the studies by Chen [18] and Mingchao [19]. Table 1 summarizes the material parameters used for the simulations conducted in this study.

2.4. Boundary Conditions

In Chen's study, both experiments and simulations were conducted to predict the fatigue life of the component under three different combined tension-torsion loading cases. The boundary conditions were defined consistently with those used in the experiments. One end of the component was fully constrained (fixed support), while the other end was subjected to an axial load and a torsional moment. For the static analysis, the first loading case was selected for comparison with the stress distribution reported in Chen's study.

2.5. Static Analysis Results

Chen's study provides the stress distribution (Fig. 4) for the defect-free CAD model under the first combined loading case. Based on these data, a comparison is conducted to validate the accuracy of the reconstructed CAD model derived from the original geometry, thereby assessing the reliability of the simulation in reproducing the actual stress state of the component.

After recalibrating the scale bar, it can be observed that the stress distribution of the reconstructed model (shown in Fig. 5) is consistent with the simulation results reported by Chen. In addition, both the location and magnitude of the maximum stress show only minor deviations and remain within an acceptable range. Specifically, the reconstructed model yields a maximum von Mises stress of 543 MPa, while Chen's simulation reports a maximum von Mises stress of 569 MPa and a maximum principal stress of 558 MPa. The discrepancies between the results range from 2.68% to 4.5%. Therefore, it can be concluded that the reconstructed CAD model is consistent with the reference model and can be reliably used for subsequent analyses in this study.

2.6. Fatigue Life Prediction Basis

Table 1. Material properties

UTS (MPa)	Density (g/cm^3)	YS (MPa)	Elastic modulus (GPa)	Poisson's ratio
1050	4.44	995	117	0.34
S–N curve	$\log N = 9.449 - 2.078 \log(\sigma_{max} - 491.5)$			

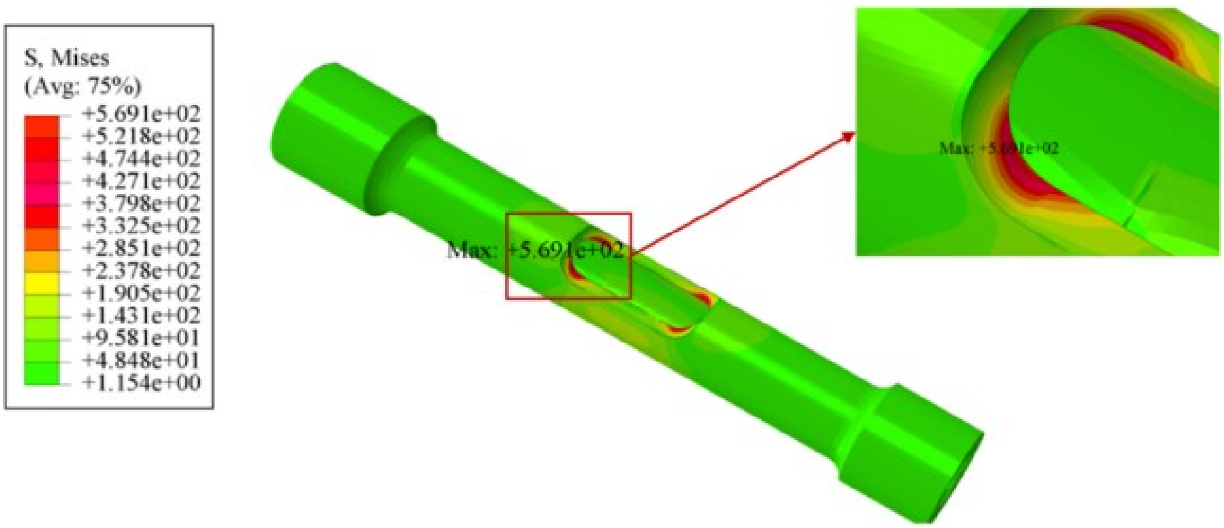

Fig. 4. von Mises stress distribution reported by Chen

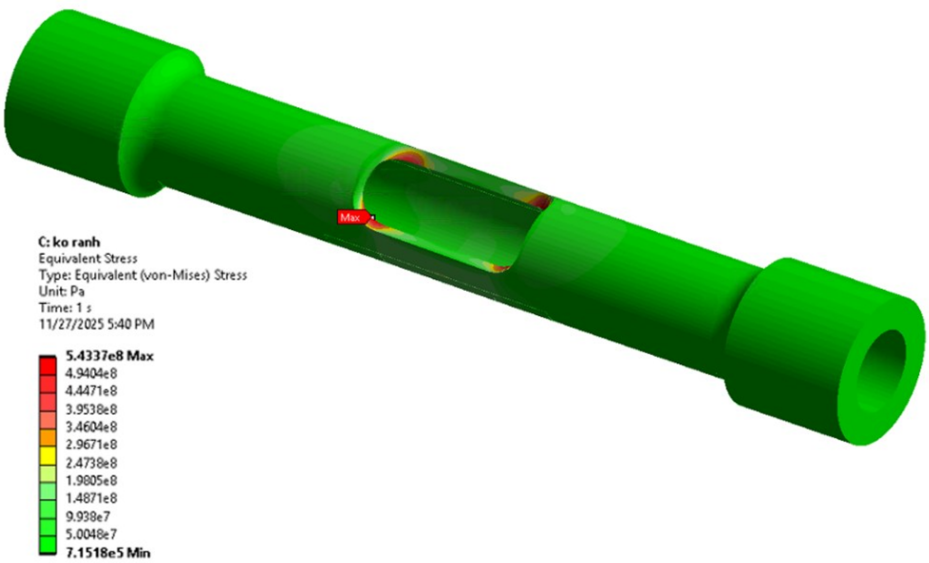

Fig. 5. von Mises stress distribution

In ANSYS Mechanical, fatigue life simulation is based on two main theoretical foundations: stress analysis using FEM and classical fatigue models, namely Stress-Life (S-N) and Strain-Life (ε-N). For high-cycle fatigue problems, the Stress-Life approach is preferred because the material primarily behaves within the elastic regime, and this approach is therefore adopted in this study. At each node of the finite element model, the stress obtained from the static analysis is mapped onto the S-N curve to determine the number of cycles to failure.

The software first performs a static stress analysis, and then uses the equivalent von Mises stress to evaluate fatigue life based on the S-N curve. For each load ratio, the maximum and minimum von Mises stresses (σ_{max} and σ_{min}) are used to calculate the stress amplitude and mean stress for fatigue assessment.

The equivalent stress is calculated according to the formulation reported by Jie Zhou [20]:

Stress amplitude and mean stress:

$$\sigma_a=\frac{\sigma_{max}-\sigma_{min}}{2} \quad (1)$$

$$\sigma_m=\frac{\sigma_{max}+\sigma_{min}}{2} \quad (2)$$

Goodman model:

$$\sigma_{a,eq}=\frac{\sigma_a}{1-\frac{\sigma_m}{\sigma_u}} \quad (3)$$

Gerber model:

$$\sigma_{a,eq}=\frac{\sigma_a}{1-\left(\frac{\sigma_m}{\sigma_u}\right)^2} \quad (4)$$

Soderberg model:

$$\sigma_{a,eq}=\frac{\sigma_a}{1-\frac{\sigma_m}{\sigma_y}} \quad (5)$$

Subsequently, ANSYS calculates the equivalent alternating stress to transform stresses under different load ratios into a single representative value. To account for the effect of mean stress in the loading cycle, correction models such as Goodman, Gerber, or Soderberg are applied.

This equivalent stress is then compared with the S-N curve to determine the fatigue life of the component. Essentially, ANSYS performs a static simulation to compute the equivalent stress, from which the fatigue life is subsequently derived. The following section presents the simulation procedure used to validate the fatigue life prediction model and algorithm proposed by Chen.

2.7. Fatigue Analysis Results of the Component

The CAD model described in Section 2.1 is further employed, with the inclusion of a defect of depth h=0.25 mm. The mesh is defined similarly to that in Section 2.2; however, the defect surface is assigned a refined element size of 0.025 mm. Fig. 6 illustrates the meshing results on the defect surface. The total number of mesh elements does not differ significantly from the defect-free case. However, due to the semi-circular profile and small size of the scratch, the meshing time increases considerably compared to the intact component. The boundary conditions are defined in the same manner as in Section 2.4. An axial load of 1943 N and a torsional moment of 76 Nm are applied to the validation model. Consistent with Chen's experiments, a load ratio of (R = 0) is adopted, and the Goodman mean stress theory is employed to evaluate the fatigue life of the component.

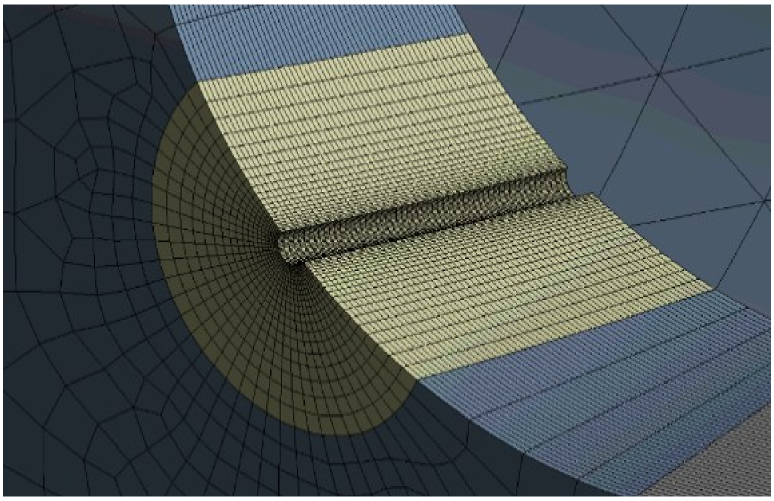

Fig. 6. Mesh at the scratch location

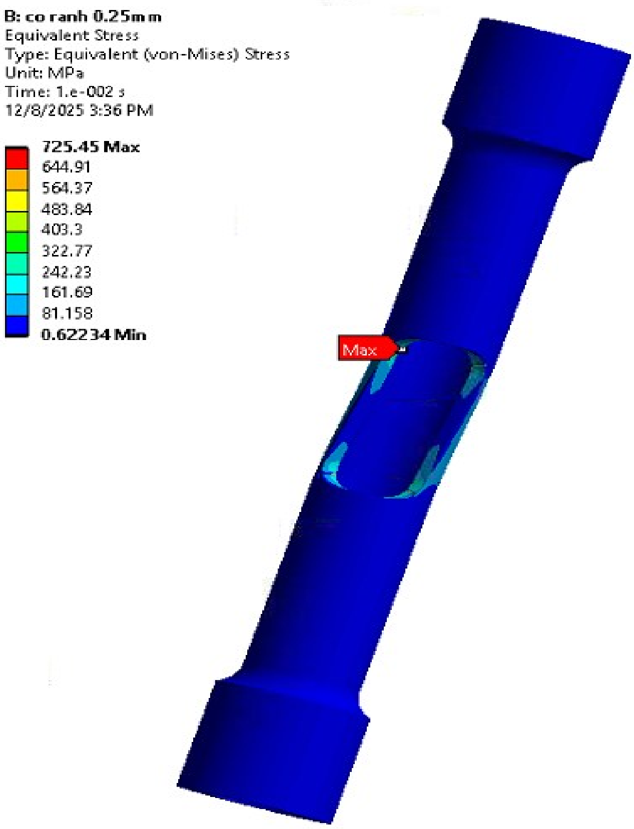

Fig. 7. von Mises stress distribution on scratched component

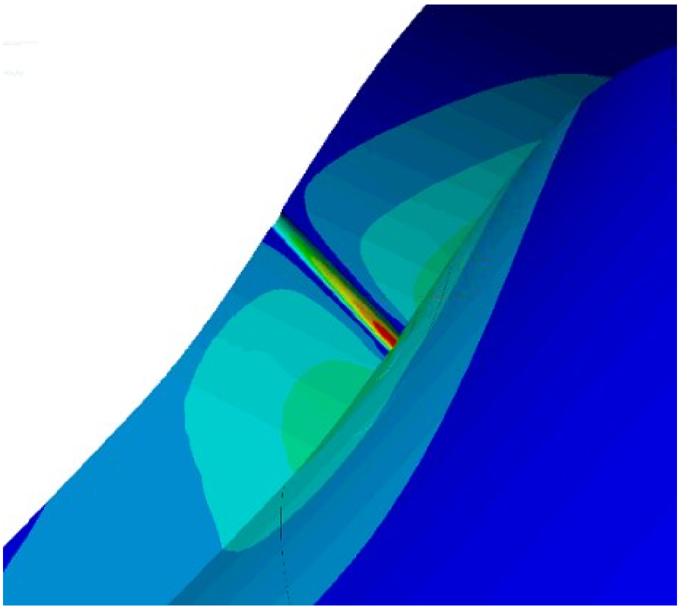

Fig. 8. Stress concentration location

Observation of the stress distribution of the component under combined tension-torsion loading in Fig. 7 and Fig. 8 shows that the deformation trend and stress concentration mechanism are fully consistent with the characteristics of a component containing a surface defect. The maximum von Mises stress reaches approximately 725 MPa and occurs at the root of the defect, where the curvature radius is smallest and acts as the primary stress concentration site. From the defect root, the stress decreases rapidly with increasing distance, reflecting the attenuation of stress concentration as the stress field transitions back to the global geometric distribution of the component. Overall, the obtained stress distribution accurately captures the stress concentration behavior and provides a reliable basis for subsequent fatigue life prediction presented in the following sections. The equivalent stress is concentrated at the defect location, indicating that this is the region most likely to initiate failure when the component exceeds its fatigue limit. The maximum equivalent stress reaches approximately 570 MPa, which is consistent with the stress concentration at the defect root and accurately reflects the degradation in strength associated with the presence of a surface defect.

Fig. 9 shows the fatigue life distribution on the component surface calculated using ANSYS Mechanical. The average fatigue life predicted by Chen's method is approximately 350,000 cycles. In comparison, the simulation results obtained in this study yield a fatigue life of 320,690 cycles, with a relative error of about 8% at the defect location. This level of discrepancy is considered acceptable, particularly given the complexity of defect modeling, the sensitivity of the stress field to defect geometry, and the influence of mesh refinement in the stress concentration region. In addition, Chen's model incorporates stress gradient correction algorithms and defect influence functions, whereas the ANSYS simulation is based solely on the stress field derived from linear analysis, which is inherently sensitive to mesh quality at the defect root.

Considering these factors, a deviation of approximately 8% is regarded as reasonable. Therefore, it can be concluded that the simulation model developed in this study is consistent with Chen's predictions and is sufficiently reliable for use in subsequent analyses.

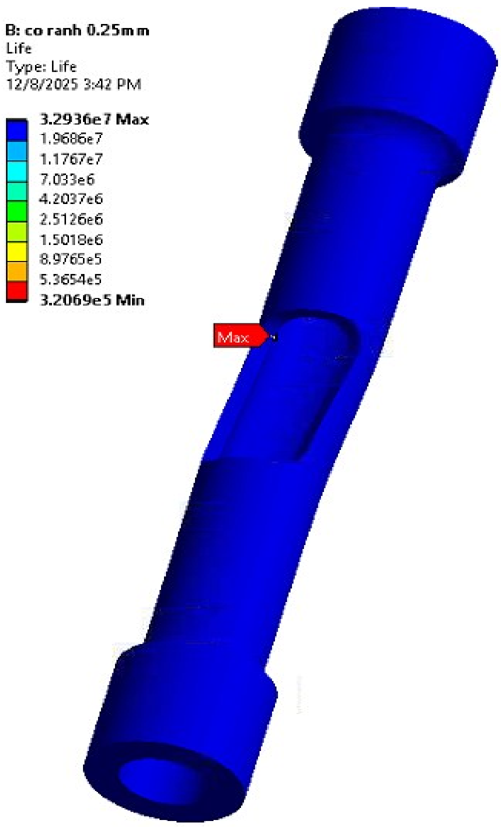

Fig. 9. Fatigue life distribution

3. Analysis of the Effect of Groove Geometry in Thin-Walled Structures on Stress and Fatigue Life

In the previous section, the fatigue life prediction model proposed by Chen et al. was reconstructed and validated for TC4 components with surface scratch defects. The simulation results show good agreement in both stress distribution and predicted fatigue life compared to the reference data, thereby confirming the reliability of the numerical model and the fatigue assessment approach employed, despite the requirement for a highly refined mesh in the stress concentration region, which leads to a large number of elements and increased computational time due to the high curvature geometry at the scratch root.

In practical applications, when surface defects or localized fatigue cracks occur, a commonly adopted approach is to remove the damaged material through machining in order to eliminate the initial crack tip [8], thereby forming dents or grooves with controlled geometry. This process alters the local geometry of the component, leading to a redistribution of the stress field and potentially affecting the remaining fatigue life. However, within the scope of this study, the objective is not to evaluate or optimize repair methods, but rather to analyze the influence of groove geometry on the predicted fatigue life associated with crack initiation. This approach has been previously discussed by Mingchao et al. [19]. Nevertheless, that study was limited to flat plate specimens and did not fully clarify the effect of surface material removal on the fatigue life of thin-walled structures. Therefore, in this section, the model is extended by introducing grooves with larger dimensions but smoother profiles compared to the initial defect, in order to systematically investigate the influence of geometric variation on stress distribution and fatigue life. The groove geometry is characterized by its depth (h) and width (w), and a dimensionless geometric parameter is introduced. Based on this, the influence of the dimensionless parameter on fatigue life is evaluated and compared across different geometric configurations. All other model parameters, including material properties, boundary conditions, loading, and fatigue assessment methodology, are kept consistent with the previous section to ensure comparability of the results.

3.1. Description of Extended Groove Geometry and the Geometric Parameter i_{AR}

Based on the validated model presented in Section 2, the defect geometry is extended by replacing the initial scratch with a groove of larger dimensions but smoother profiles. The groove is assumed to extend longitudinally through the entire thickness of the component. The overall geometry of the component, material properties, boundary conditions, and applied loading are kept unchanged. The extended groove geometry is illustrated in Fig. 10 and is characterized by two main parameters: the groove depth h (measured normal to the surface) and the groove width w (measured parallel to the component surface). The investigated cases are selected such that the grooves have larger overall dimensions than the initial defect, with the expectation of producing a lower level of stress concentration at the groove root.

To facilitate comparison and trend analysis of the influence of groove geometry on fatigue life, a dimensionless geometric parameter, denoted as i_{AR}, is introduced and defined as follows:

$$i_{AR}=\frac{w}{h} \tag{6}$$

The parameter i_{AR} represents the relative relationship between the lateral expansion and the normal penetration depth of the groove. The use of this parameter enables a quantitative evaluation of the influence of groove geometry on the stress field and fatigue life, while eliminating the effect of absolute size when comparing different cases.

Within the scope of this study, different values of i_{AR} are selected by systematically varying the groove width and depth, while maintaining the groove location and all other simulation parameters unchanged. On this basis, the influence of i_{AR} on the local stress distribution and the predicted fatigue life of the crack is analyzed and discussed in the following section.

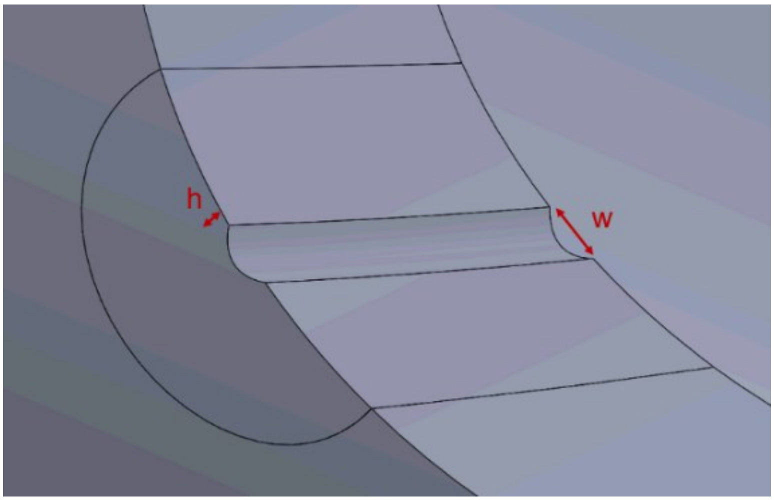

Fig. 10. Groove geometry

i_{AR}	von Mises stress distribution
2.17	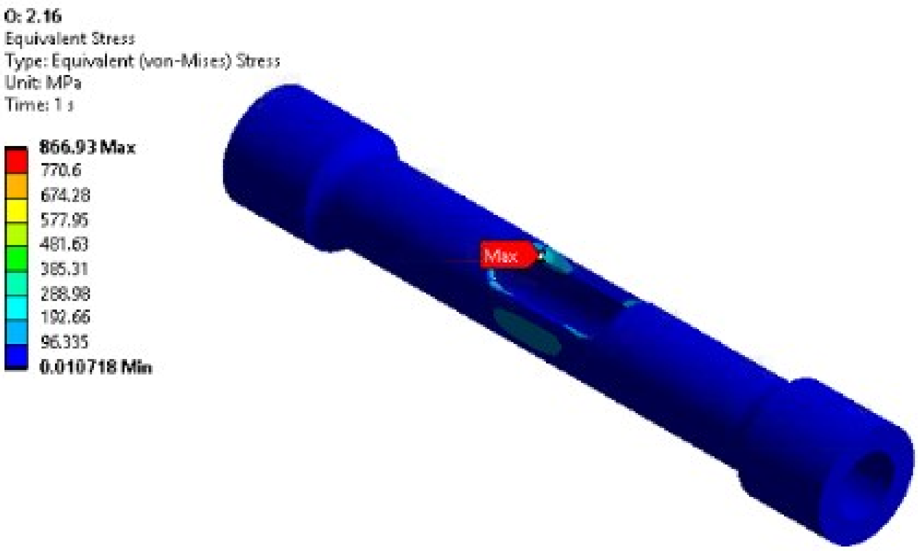
2.5	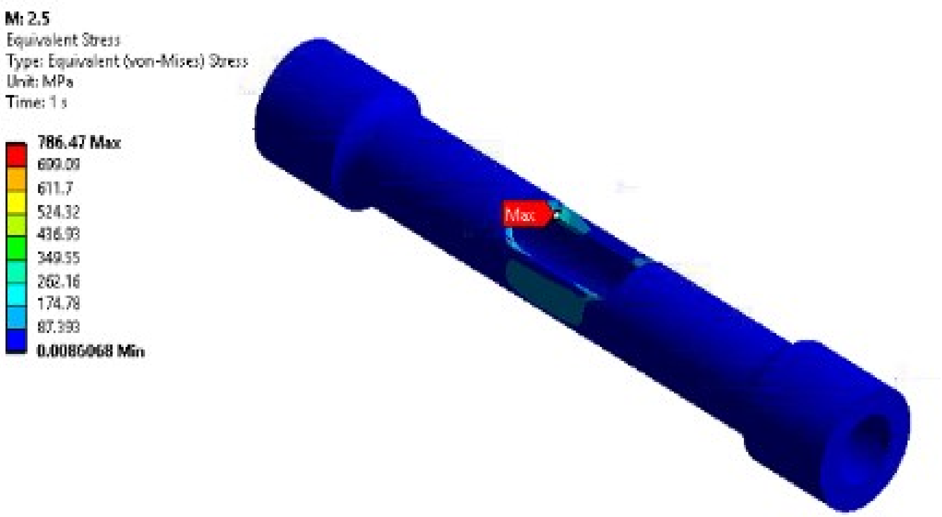

Fig. 11. von Mises stress distribution for different i_{AR}

i_{AR}	von Mises stress distribution
2.6	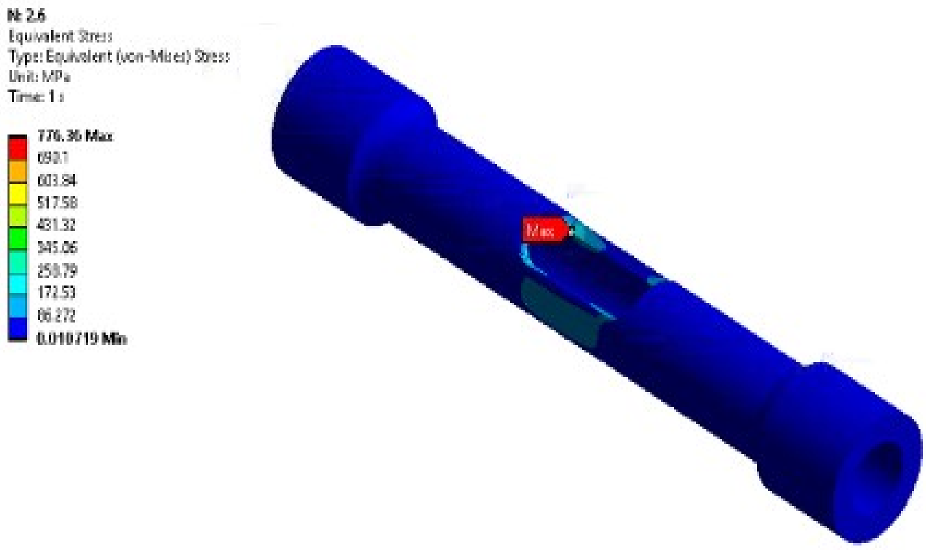
2.8	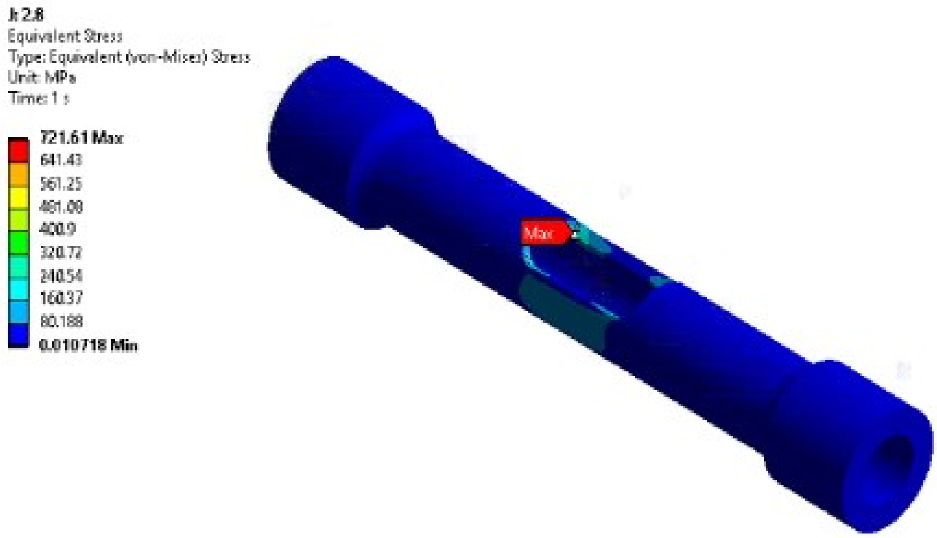
3	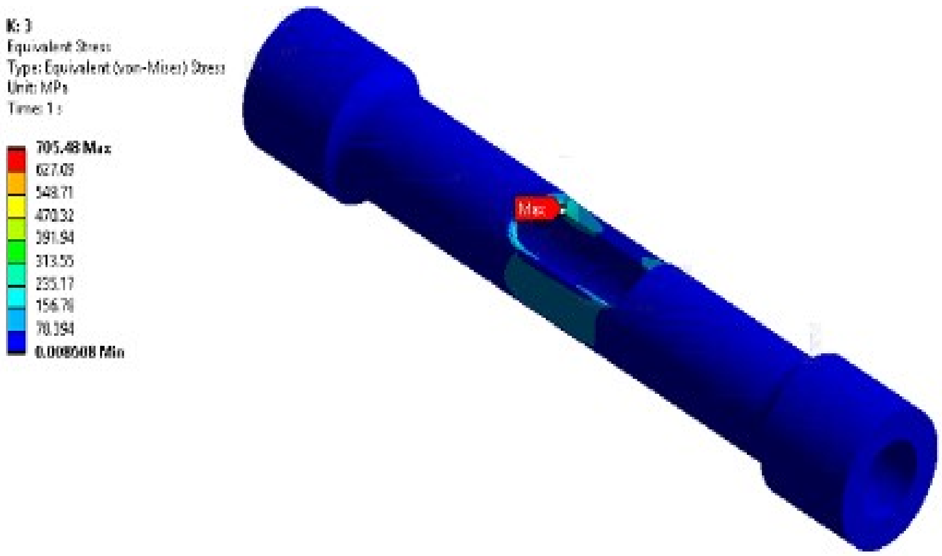

Fig. 11. (continued)

i_{AR}	von Mises stress distribution
3.3	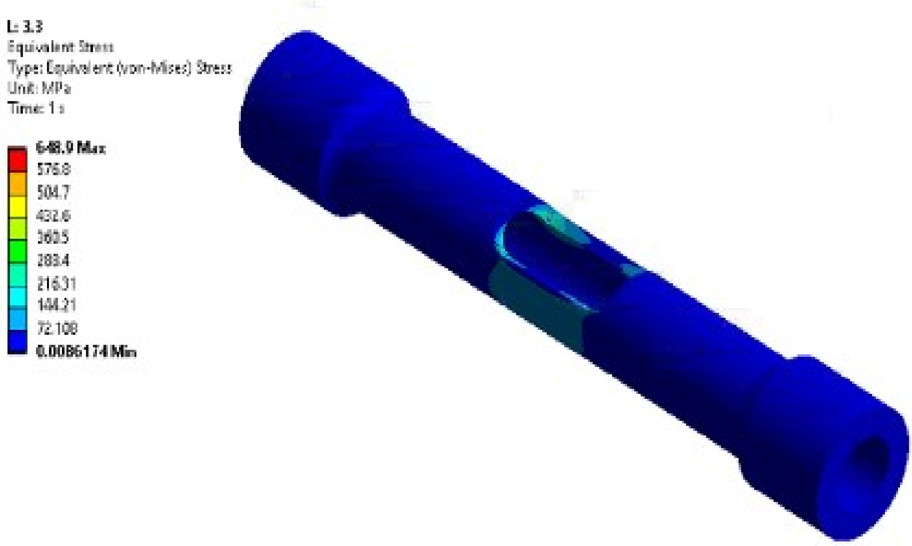

Fig. 11. (continued)

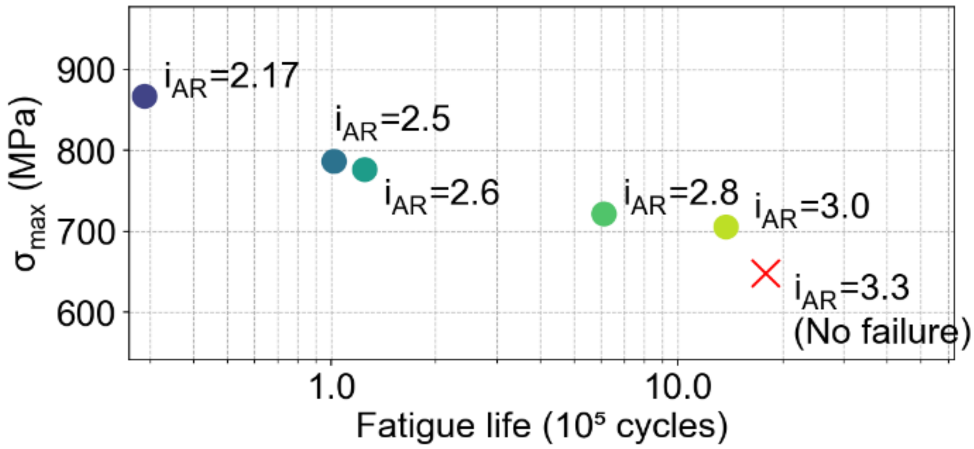

Fig. 12. Fatigue life for different iAR values

3.2. Simulation Setup

The finite element model setup in this section follows the same procedure as the validation of Chen et al.'s model, including material modeling, boundary conditions, loading conditions, and the fatigue life assessment method. The only difference among the investigated cases lies in the defect geometry, which is replaced by extended grooves with profiles as described in Section 3.1. Maintaining consistent assumptions and simulation parameters ensures comparability and enables direct comparison between the results.

3.3. Effect of the i_{AR} Parameter on Stress Distribution and Fatigue Life

Based on the groove geometry described in Section 3.1, the characteristic parameters are used to derive the i_{AR} index. The groove depth is limited from the initial defect depth up to 0.3 mm, while the groove width ranges from 0.65 mm to 1.25 mm, resulting in i_{AR} values between 2.17 and 3.3. The von Mises equivalent stress field in the groove region is extracted and analyzed for different i_{AR} cases. The results show that the maximum stress region consistently appears at the root of the semi-elliptical groove, which is consistent with the stress concentration mechanism and fatigue crack initiation location observed in the model validation section.

Fig. 11 illustrates the von Mises stress distribution for several representative i_{AR} cases. Observation of the stress contours indicates that the maximum stress location in all cases is at the groove root. As i_{AR} increases, the stress field in the groove region tends to become more uniformly distributed, and the stress gradient becomes smoother, reflecting the transition toward a gentler groove geometry. Notably, for cases with i_{AR}<2.7, although the stress distribution becomes more uniform compared to the initial deep defect, the maximum stress at the groove root remains higher than that of the original defect with depth h=0.25 mm. This indicates that increasing the groove width in the low i_{AR} range is not sufficient to compensate for the adverse effect of groove depth on local stress concentration.

Based on the maximum values obtained from the von Mises stress field, as discussed in Section 3, the fatigue life results of the component for different i_{AR} values are presented in Fig. 12. As i_{AR} increases from 2.17 to 3.3, the maximum von Mises stress at the groove root decreases significantly from 866.9 MPa to 648.9 MPa, leading to a substantial increase in fatigue life.

For low i_{AR} values (2.17-2.6), although the groove geometry becomes smoother compared to the initial deep defect, the maximum stress remains high, resulting in very low fatigue life, ranging from 0.29×10^5 to 1.25×10^5 cycles. These values are significantly lower than the initial fatigue life of the component (3.2×10^5 cycles), indicating that in the low i_{AR} range, enlarging the groove geometry does not improve fatigue life and may even reduce the original fatigue performance of the component.

When i_{AR} exceeds 2.7, the maximum stress decreases significantly to below 730 MPa, while the fatigue life increases rapidly in a nonlinear manner. Specifically, at i_{AR}=2.8 and 3.0, the fatigue life reaches 6.12×10^5 and 13.76×10^5 cycles, respectively, far exceeding the initial fatigue life of the component. This indicates that a sufficiently smooth groove geometry can substantially reduce stress concentration and significantly improve fatigue resistance.

In particular, at (i_{AR}=3.3), no fatigue failure is observed because the equivalent stress is below the fatigue limit of the material. This indicates that the local stress has decreased below the fatigue threshold according to the Goodman criterion adopted in this study. This result confirms that i_{AR} is a dominant parameter governing fatigue life, and that there exists a sufficiently large i_{AR} range in which the fatigue life of the component is not only restored but also exceeds its initial value.

4. Conclusion

In this study, the fatigue life prediction simulation proposed by Chen et al. was reconstructed in ANSYS to validate the accuracy of the numerical simulation approach. The static stress analysis results for the defect-free component show deviations in the range of 2.7-4.5% compared to the published data. When a surface scratch defect with a depth of 0.25 mm is introduced into the simulation, the stress field exhibits a pronounced concentration at the scratch root, consistent with the fatigue crack initiation mechanism reported in previous studies. Compared with the fatigue life predicted by Chen's simulations, the discrepancy of approximately 8% is considered acceptable.

Based on the validation results, the study is further extended to investigate the effect of extended groove geometry in thin-walled structures on stress distribution and fatigue life through the dimensionless geometric parameter i_{AR}. The results show that as i_{AR} increases, the maximum von Mises stress at the groove root decreases significantly, while the fatigue life increases in a nonlinear manner. For i_{AR}<2.7, although the stress distribution becomes more uniform, the fatigue life remains lower than that of the initial component.

The identified threshold of i_{AR}=2.7 can therefore be considered a practical design guideline for improving the fatigue performance of TC4 thin-walled structures. Below this value, stress concentration remains pronounced, resulting in reduced fatigue life, whereas higher i_{AR} values effectively reduce stress concentration and enhance durability. Consequently, controlling the groove geometry through the i_{AR} parameter provides a simple and effective strategy for fatigue life recovery. Future work should include experimental validation to confirm the numerical results and further support the proposed mechanism.

Although improving fatigue life in practice through modification of defect geometry may require corresponding adjustments to other system components to satisfy operational requirements, the proposed evaluation in this study clearly demonstrates the dominant role of groove geometry, characterized by the i_{AR} parameter, in governing fatigue behavior. Future research may extend the present geometry-based fatigue-life assessment to other material systems, including aeronautical composite laminates, where damage-based crack-growth prediction using iso-damage curves has been demonstrated by Hoang et al. [21].

Acknowledgments

The authors gratefully acknowledge the support of Singapore Institute of Technology and Hanoi University of Science and Technology during this research.

Declaration of Generative AI

During the preparation of this work, the authors used ChatGPT to improve the language and presentation of the manuscript. The authors reviewed and verified all AI-assisted content for accuracy and made the necessary edits. The authors take full responsibility for the final content of the published article.

References

[1] A. Mote, T.E. Lacy, J.C. Newman. (2024). Assessing fatigue crack growth thresholds for a Ti-6Al-4V (STOA) alloy using two experimental methods. *Engineering Fracture Mechanics*, 301, 110006. https://doi.org/10.1016/j.engfracmech.2024.110006

[2] V. Sinha, C. Mercer, W.O. Soboyejo. (2000). An investigation of short and long fatigue crack growth behavior of Ti-6Al-4V. *Materials Science and Engineering: A*, 287(1), 30-42. https://doi.org/10.1016/S0921-5093(00)00817-0

[3] J. Zhang, S. Yang, J. Lin. (2015). Fatigue crack growth rate of Ti-6Al-4V considering the effects of fracture toughness and crack closure. *Chinese Journal of Mechanical Engineering*, 28, 409-415. https://doi.org/10.3901/CJME.2015.0104.002

[4] G. Ping, Z. Yongqing, Z. Weidong. (2015). Fatigue crack growth behavior in TC4-DT titanium alloy with different lamellar microstructures. *Rare Metal Materials and Engineering*, 44(2), 277-281. https://doi.org/10.1016/S1875-5372(15)30019-9

[5] S.R. Stock, M.A. Langøy. (2001). Fatigue-crack growth in Ti-6Al-4V-0.1Ru in air and seawater: Part I. Design of experiments, assessment, and crack growth-rate curves. *Metallurgical and Materials Transactions A*, 32, 2297-2314. https://doi.org/10.1007/s11661-001-0204-9

[6] T. Li, H. Liu, D. An, Q. Hu, X. Xu, X. Li, J. Chen. (2024). Achieving excellent fatigue crack growth resistance and tensile strength combination in multilayered TC4/TB8 structures. *Vacuum*, vol. 222, 113067. https://doi.org/10.1016/j.vacuum.2024.113067

[7] J. Liu, J. Li, F. Jin, D. Zhang, W. Guo, J. Xiong. (2025). Macro and micro structural responses of dissimilar TC4/TC17 titanium alloy joints in linear friction welding and post-welding heat treatment processes and their effects on tensile and fatigue performance. *Journal of Materials Research and Technology*, 37, 484–492. https://doi.org/10.1016/j.jmrt.2025.06.049

[8] P. Li, S. Wang, J. Wu, Y. Shen, Z. Dong, H. Xu. (2026). Ultrasonic surface rolling process for improving fatigue crack propagation resistance

of laser-clad TC4-TA15 titanium alloy. *Surface and Coatings Technology*, 520, 132974. https://doi.org/10.1016/j.surfcoat.2025.132974

[9] T. Li, X. He, W. Deng, Z. Li, L. Han. (2026). Fatigue crack growth behavior and mechanisms of diffusion-bonded TC4/TC21 laminates. International Journal of Fatigue, 209, 109590. https://doi.org/10.1016/j.ijfatigue.2026.109590

[10] G. Jiayuan, C. Jiahui, Z. Song, Z. Zhichao, G. Shoulong, L. Zhou. (2025). Effect of ultrasonic rolling on crack growth behavior of TC4 titanium alloy laser weld under overload condition. *Theoretical and Applied Fracture Mechanics*, 138, 104910. https://doi.org/10.1016/j.tafmec.2025.104910

[11] P. Zhang, Y. Gao, Y. Yu, Y. Sun, H. Zhou, J. Zhang. (2025). Effects of water-guided laser surface strengthening on surface properties and fatigue life of TC4 titanium alloy in tension-tension fatigue tests. *Vacuum*, 232, 113863. https://doi.org/10.1016/j.vacuum.2024.113863

[12] V. Bonu, K. Barat, M. Jeevitha, Siju, N. Jagannathan, H.C. Barshilia. (2025). Influence of erosion damage on high-cycle fatigue failure mechanism of uncoated and erosion-resistant nanolayered multilayered TiCr/TiCrN coated Ti6Al4V. *Surface and Coatings Technology*, 518, 132909. https://doi.org/10.1016/j.surfcoat.2025.132909

[13] S. Li, Q. Liu, H. Li, W. Wang, R. Lu, X. Ruan, Y. Wang, Y. Meng, H. Chen. (2026). A microcrack evolution-based fatigue damage model for assessment of laser-arc hybrid welded joints in TC4 titanium alloy. *International Journal of Fatigue*, 202, 109231. https://doi.org/10.1016/j.ijfatigue.2025.109231

[14] Z. Lei, L. He, R. Liu, X. Zhao. (2026). Fatigue crack initiation mechanism and life prediction of laser-arc hybrid welded TC4 titanium alloy joints. *International Journal of Fatigue*, 203, 109308. https://doi.org/10.1016/j.ijfatigue.2025.109308

[15] H. Deng, J. Liu, H. Kang, Y. Guo, L. Song, H. Yu. (2025). Very high cycle fatigue behavior of TC4 titanium alloy: Faceting cracking mechanism and life prediction based on dislocation characterization. *International Journal of Fatigue*, 190, 108640. https://doi.org/10.1016/j.ijfatigue.2024.108640

[16] Y. Wang, S. Yu, W. Peng, N. Li, C. Zhao, J. Liu, Z. Chen, L. Wang, W. Li, Q. Wang. (2026). The analysis of fracture toughness and fracture mechanisms of TC4 alloy at different temperatures. *Materials Today Communications*, 51, 114622. https://doi.org/10.1016/j.mtcomm.2026.114622

[17] X. CHEN, Y. ZHAO, C. ZHAO, X. YE, W. XU, Y. HE. (2024). Flaw tolerance performance of TC4 alloy used in transmission system. *Journal of Aeronautical Materials*, 44(2), 169-175. https://doi.org/10.11868/j.issn.1005-5053.2023.000196

[18] X. Chen, W. Hu, Y. Zeng, J. Li, D. Zhang, X. Zhan, Q. Meng. (2026). A damage mechanics-based fatigue life prediction method for TC4 components considering combined influence of scratch defects and structural geometric features. *International Journal of Fatigue*, 203, 109319. https://doi.org/10.1016/j.ijfatigue.2025.109319

[19] M. Ding, Y. Zhang, B. Li, C. Sun, H. Lu, W. Liu. (2022). Total fatigue life prediction of TC4 titanium alloy based on surface notch. *Engineering Failure Analysis*, 131, 105868. https://doi.org/10.1016/j.engfailanal.2021.105868

[20] J. Zhou, H.-Z. Huang, B. Zheng, Z. Peng. (2017). Fatigue Life Prediction Based on Walker and Masson Models. *Proceedings of the Asia Pacific Conference of the PHM Society 2017, PHM Society Asia-Pacific Conference, 1(1), 371-378*. https://doi.org/10.36001/phmap.2017.v1i1.1818

[21] N.T. Hoang, D. Gamby, M.-C. Lafarie-Frenot. (2010). Predicting fatigue transverse crack

growth in cross-ply carbon–epoxy laminates from quasi-static strength tests by using iso-damage curves. *International Journal of Fatigue*, 32(1), 166–173. https://doi.org/10.1016/j.ijfatigue.2009.02.045